

applied to the inter-atomic potential of Si-Si and the ZBL model [11] is applied to B-B and B-Si. A Si (001) substrate is considered consisting of 32768 atoms with a cube side of about 90Å. Periodic boundary conditions are applied to the (100) and (010) boundaries and the atoms in lowest layer are fixed to retain the bulk structure. Before implantation of a B monomer/cluster, the substrate is heated to 300K and the top surface is reconstructed to 2×1 structure. In this work, B₄ and B₁₀ are irradiated with a different geometry as shown in Fig. 1. Because, as the cluster size decreases, the structure and orientation of the cluster at impact becomes more significant, whereas large clusters have a spherical structure and no dependency of orientation. In the case of B₄, two cluster structures were considered; one has a square structure and the other a chain structure, and each B₄ cluster impacts parallel and perpendicular direction to the Si surface. A B₁₀ cluster is implanted as a horizontal chain, a vertical chain and a spherical f.c.c. structure. The distance between the B atoms is 1.8Å for each structure which was calculated from the atomic radius of a boron atom. B₁ monomer and vertical B₄ and B₁₀ chains are implanted with an incident angle of 7° to the surface normal and rotated 30° to the {001} direction to avoid channeling implantation, and other clusters are implanted with normal direction. In order to obtain statistical properties, such as depth profile of implant atoms and displacements, 100 simulations for B₁ and 25 simulations for both B₄ and B₁₀ were done at different impact points, respectively.

III. RESULTS AND DISCUSSION

A. Implant Efficiency and Profile of Boron Atoms

Figs. 2(a)-2(c) show the depth profiles of implanted B atoms from B₁, B₄ and B₁₀, respectively, 1.2ps after impact. The region on the RH side where the depth is larger than 0Å indicates the substrate and the values on the LH side indicate the ratio of unimplanted boron atoms to the total irradiated atoms. B₁, B₄ and B₁₀ are irradiated on the target with the same incident energy of 230eV/atom so that the total incident energy of B₄ and B₁₀ is 0.92keV and 2.3keV, respectively. B₄ and B₁₀ implantation shows the same implant efficiency as B₁ of about 82%, except for the case of the vertical B₄ and B₁₀ chains. In these cases, almost all B atoms are implanted into the substrate without all colliding with the substrate atoms. It is considered that the first B atom of a chain cluster knocks-on a substrate Si atom and the following B atoms can penetrate to deeper regions. However, the implant efficiency of square B₄ clusters shows a similar value as that of B₁ and the horizontal B₄ chain cluster. This result suggests that the stack number of two in a B₄ square is not enough density to cause an improvement in implant efficiency, but four is enough for this incident energy of 230eV/atom. This assumption is supported by the spherical B₁₀ in which the stack number is two or three and shows similar implant efficiency to that of a horizontal B₁₀ chain rather than a vertical B₁₀ chain. From the viewpoint of the implant profile, there is no significant difference among the B₄ clusters, almost all B₁₀ and the B₁ monomer, but only the vertical B₁₀ chain cluster shows a deeper profile compared with the other implant profiles. In the case of the vertical B₄ chain cluster impact, the B₄ cluster collapses immediately after it penetrates the first layer of the substrate. However, the B₁₀ chain keeps

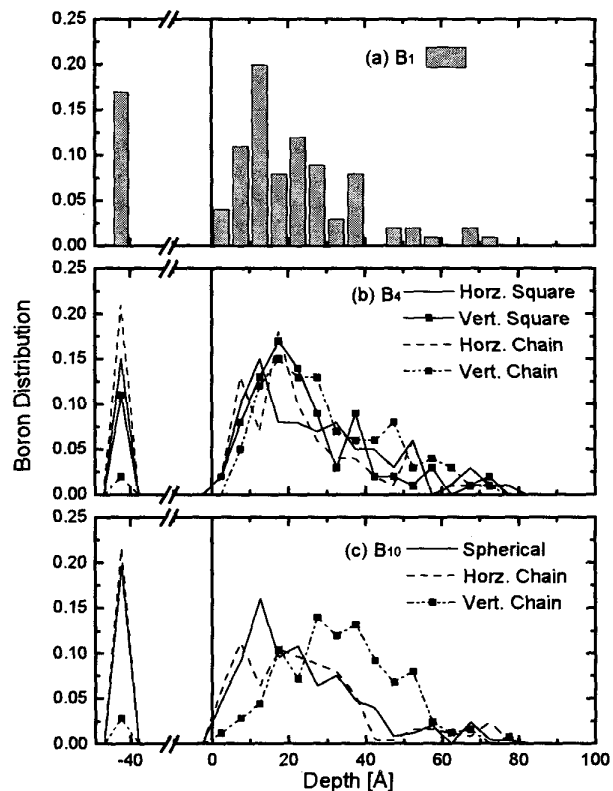


Fig. 2: Implant profile of B atoms by (a) B₁, (b) B₄ and (c) B₁₀ implantation. The depth of 0Å shows the surface of the substrate and the values on the left side indicate the ratio of unimplanted B atoms to total irradiated atoms. Note that the ratios of unimplanted atoms by vertical chain-like B₄ and B₁₀ are reduced.

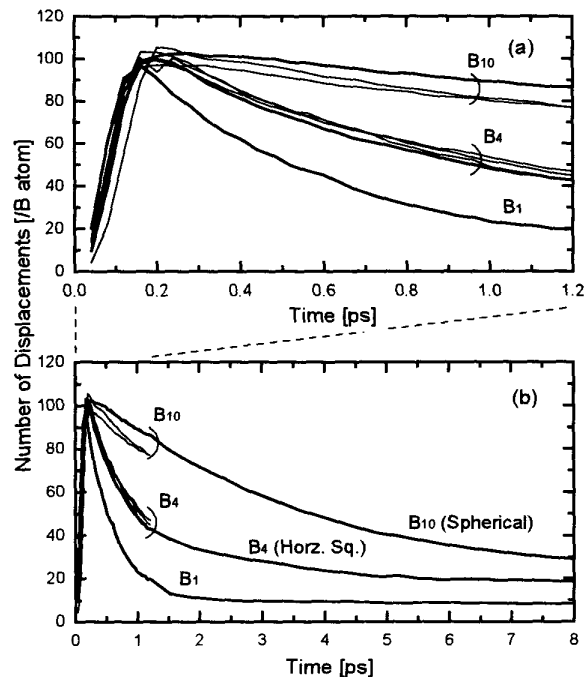


Fig. 3: Time transition of the number of displacements induced by boron monomer and clusters. Fig. 3(a) shows the results for every variation of monomer/cluster until 1.2ps and Fig. 3(b) shows the following results of B₁, horizontal B₄ square and spherical B₁₀ cluster until 8ps.

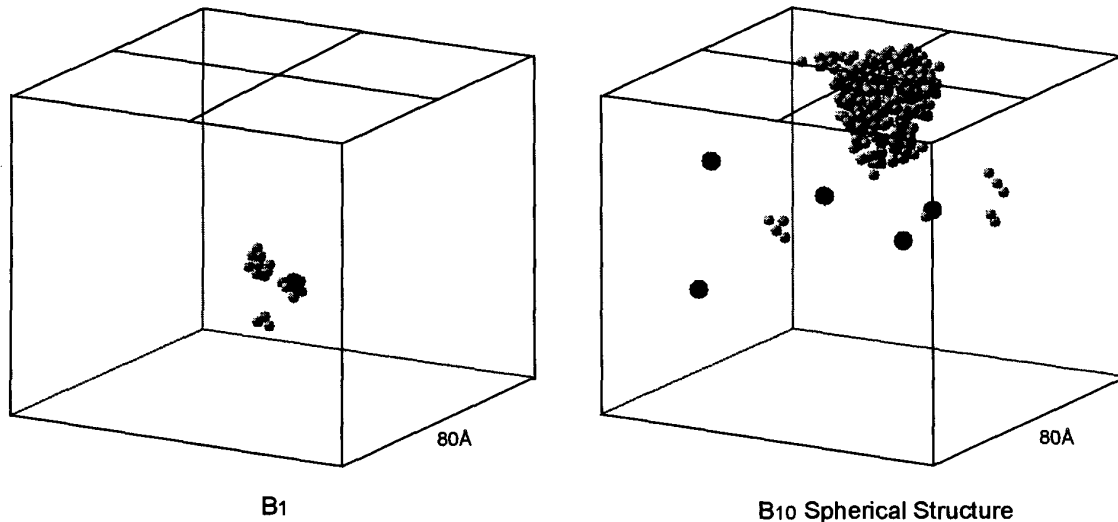


Fig. 4: Snapshots of B_1 monomer and B_{10} cluster implanted with 230eV/atom, 8ps after impact. Black spheres represent the implanted B atoms and gray ones are displaced Si atoms.

the coherency of velocity in the substrate and each B atom continues to penetrate deeply into the substrate. When the interaction between the incident B atoms is less probable, as in the cases of a chain or a spherical B_{10} cluster, each B atom in the cluster acts in a way similar to monomer ions with the same energy per atom. The result of implant efficiency and implant profiles are in agreement with the experimental results that $B_{10}H_{14}$ which has spherical structure and shows the same implant profile as B monomer ions accelerated with 1/10 of the energy of $B_{10}H_{14}$ [5]. These experimental and MD results demonstrate that each B atom in $B_{10}H_{14}$ can be treated as independent B monomer ions.

B. Damage Formation by Boron Cluster Impact

Fig. 3(a) and Fig. 3(b) show the time dependence of the number of displacements per single B atom. The displacements are defined as the Si atoms which have a potential energy of 0.4eV above the bulk state [12]. Fig. 3(a) shows the transition of the displacement yield by B_1 monomers and various B_4 and B_{10} clusters from 0ps to 1.2ps. Fig. 3(b) shows the results from the calculation continued on to 8ps for B_1 , horizontal B_4 square and spherical B_{10} . Until the time of 0.2ps, almost all of the incident energy from initial B atoms is transferred to substrate atoms, and the number of displacements reaches the maximum value at around 0.2ps and then decreases. The maximum number of displacements depends neither on cluster size nor on cluster structure. It is considered that each implanted B atom interacts with the substrate atoms individually and the kinetic energy of the incident atoms is transferred to the substrate without overlapping. This suggestion agrees with the aforementioned result that implant profile and implant efficiency does not have size and structure dependency except for the case of the vertical chain cluster. The damage recovery process is different depending on the cluster size. As shown in Fig. 3(b), the displacements induced by B_1 recover rapidly in 2ps and

about eight displacements remain 8ps after impact. However, the damage recovery speed becomes slower as the cluster size increases. In the case of spherical B_{10} impact, about 30 displacements, which is four times higher than B_1 , remain 8ps after impact. The high yield displacement by cluster ion impact is due to the high-density energy irradiation effect. When a B_{10} cluster impacts the substrate, B_{10} deposits its incident kinetic energy of 2.3keV in a finite region on the surface so that a large number of energetic knocked-on atoms are created. These knocked-on atoms interact with each other, and then, these are considered to remain as the deformation of lattice in the substrate. Therefore, the yield of displacement by B_{10} remains several times higher than that of B_1 .

C. Advantages for Shallow Junction Fabrication

Fig. 4 shows snapshots of B_1 and spherical B_{10} cluster implantation into Si (001) substrate 8ps after impact. Black spheres represent the implanted B atoms and gray ones are the displaced Si atoms. Fig. 5 shows the depth profiles of displacements induced by B_1 , horizontal B_4 and spherical B_{10} cluster. The depth profiles in Fig. 5 are calculated by averaging the results of 50 trials for B_1 and of 25 trials for B_4 and B_{10} , respectively. Fig. 4 and Fig. 5 indicate that large number of displacements are formed by B_{10} compared with B_1 , as indicated in Fig. 3. Furthermore, B_1 monomer and B_{10} clusters show a difference in the distribution of displacements. In the case of B_1 implantation, transient displacements are formed along the trajectory of incident atom, however, these displacements easily recover because the deposited energy through interaction with incident atom is small. In this case, knocked-on displacements reside around the incident B atom, which is termed 'end-of-range' damage [13] as shown in Fig. 4. The end-of-range displacement is also statistically observed in the region deeper than 30Å in Fig. 5, which shows larger ratio of displacements for B_1 compared to those of B clusters. The end-of-range displacements tend to kick-out the boron

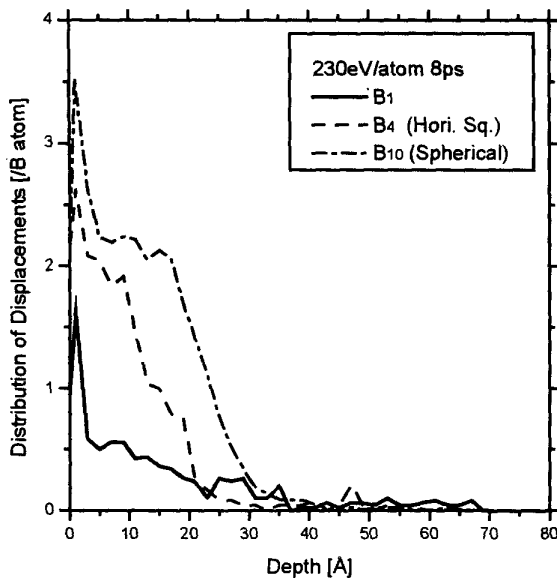


Fig. 5: Depth profile of displacements induced by B_1 monomer, horizontal B_4 square and spherical B_{10} clusters 8ps after impact.

atom from a lattice site through annealing and, therefore, the kicked-out B atom diffuses into the deeper region of substrate. This diffusion mechanism, called 'Transient Enhanced Diffusion (TED)' is a serious problem in high-quality shallow junction formation using conventional monomer ion implantation techniques [4,13]. On the other hand, B_{10} cluster creates a high density of displacements on the surface of the impact point because of the high-density energy irradiation effect. This region damaged by B_{10} is considered to be amorphized and shows a box-like shape from the surface to the depth of 20Å, which is comparable with the mean implant depth of the B atoms. This characteristic damage formation by B_{10} is expected to result in great advantages in shallow junction formation because of reducing TED without pre-amorphization process. Through annealing, the reconstruction of a substrate irradiated with B_{10} clusters proceeds from the bottom of the amorphized layer to the surface of the substrate. Therefore, the interstitial Si atom tends to move to the top surface thus avoiding B atom diffusion into deeper regions of the substrate. It has been observed experimentally that low-energy $B_{10}H_{14}$ implantation into a Si substrate does not cause TED [6,14], in a similar manner to the B implantation into a well pre-amorphized Si substrate.

IV. CONCLUSIONS

In order to examine the advantages of cluster ion implantation for high-quality shallow junction formation, molecular dynamics simulations of B_1 , B_4 and B_{10} implanting into the Si substrate were performed. It was found that B_{10} and B_4 are equivalent to 1/10 and 1/4 low-energy ion implantation, respectively. Each B atoms in the B_4 and B_{10} clusters act individually and both B types of implantation show similar implant efficiency and implant profiles to that of B_1 , except for the impact of the chain-like structure in orientation perpendicular to the substrate. The enhancement of implant efficiency was shown through the impact of

vertical chain-like clusters, whose size is larger than four because of coherency of incident velocity. For each case of impact, the number of displaced Si atoms reaches the same maximum value, but decays with different speed. The similarity in the maximum number of displacements is caused by the individuality of the incident B atoms, that is, the kinetic energy of each B atoms is transported to the displacements individually without overlapping. The decay speed is lower as the cluster size is larger because of the high-density energy irradiation effect. B_{10} deposits 10 times higher energy in finite region on the surface compared to B_1 and creates many energetic knocked-on Si atoms. These energetic substrate atoms remain as displacements on near surface region of the impact point. Therefore, the impact point is well-amorphized by cluster ion impact and this damage region is expected to stop TED of boron atoms to deeper regions of the substrate. These MD results suggests that the cluster ion implantation technique using $B_{10}H_{14}$ has great advantages for high-quality shallow junction formation through of low-energy implantation and by suppressing TED as a result of high-yield damage formation.

REFERENCES

- [1] "National Technology road Map for Semiconductors", Semiconductor Industry Association, 1997.
- [2] M.I.Current, D.Lopes, M.A.Foad, J.G.England, C.Jones and D.Su, *J. Vac. Sci. Technol.* B16(1), pp. 327-333, 1998
- [3] S.Moffatt, *Nucl. Instr. and Meth.*, B96, p. 1, 1995
- [4] H.U.Jäger, *J. Appl. Phys.* 78(1), pp. 176-186, 1995
- [5] K.Goto et al, *IEEE Tech. Dig.*, pp. 471-474, 1997
- [6] K.Goto et al, *IEEE Tech. Dig.*, pp. 435-438, 1996
- [7] T.Aoki, J.Matsuo, Z.Insepov and I.Yamada, *Nucl. Instrum. & Meth.*, B121, pp. 49-52, 1997.
- [8] T.Seki, T.Kaneko, D.Tkauchi, T.Aoki, J.Matsuo, Z.Insepov and I.Yamada, *Nucl. Instrum. & Meth.*, B121, pp. 498-502, 1997.
- [9] T.Aoki, T.Seki, J.Matsuo, Z.Insepov and I.Yamada, *Mats. Chem. & Phys.*, 54(1-3), pp. 139-142, 1998.
- [10] F.H.Stillinger and T.A.Weber, *Phys. Rev. B*, B31, p. 5652, 1985.
- [11] J.F.Ziegler, J.P.Biersack and U.Littmark, "The stopping and range of ions in solids", Pergamon Press, New York, 1985, p.321.
- [12] M.J.Caturla, T.díaz de la Rubia and G.H.Gilmer, *Nucl. Instrum. & Meth.* B196, p. 1, 1995.
- [13] K.S.Jones, P.G.Elliman, M.M.Petravic and P.Kringhoj, *Appl. Phys. Lett.* 68(22), p. 3111, 1996
- [14] T.Kusaba et al, "The boron diffusion in ultra low-energy (<1keV/atom) decaborane ($B_{10}H_{14}$) Ion Implantation", in this issue.